The 5^{th} IVS General Meeting Proceedings, 2008, p. 361–370

Progress in Technology Development
and the Next Generation VLBI System

Modeling Tropospheric Delays with Atmospheric Turbulence Models

Tobias Nilsson, Rüdiger Haas

Department of Radio and Space Science, Chalmers University of Technology, Onsala Space Observatory, Sweden

Abstract. In this work we show how atmospheric propagation delays for radio signals can be simulated based on the theory of atmospheric turbulence. We also discuss how to obtain station specific parameters, e.g. the refractive index structure constant C_n, from analysis of high resolution radiosonde data. As an example, atmospheric delays for the station Gilmore Creek and the CONT05 campaign are simulated.

1. Introduction

Atmospheric turbulence causes small scale fluctuations in the refractive index of air. These fluctuations cause variations in the atmospheric propagation delay of radio signals. Such variations are an important error source for space geodetic techniques, such as VLBI.

One way to assess how much the atmospheric turbulence degrades the accuracy of the parameters estimated in VLBI data analysis is to use simulations. The propagation delay of the VLBI signals in the neutral atmosphere can be simulated using the method presented in [1]. This approach requires knowledge of the magnitude of the turbulent variations in the refractive index. This magnitude can be described using the refractive index structure constant C_n. This parameter varies both in time and as function of location. The C_n parameters can be measured using a number of different techniques, for example using high resolution radiosonde data [2–5].

In this work we first describe in Sec. 2 how to simulate atmospheric delays, as well as how to obtain C_n using high resolution radiosonde data. In Sec. 3 we present C_n profiles obtained from radiosonde data from a number of high resolution radiosonde stations in order to investigate the variability of C_n between different climate regions as well as with season. In Sec. 4 we simulate atmospheric delays for the VLBI station Gilmore Creek, Alaska, using C_n profiles estimated using radiosonde data obtained from a nearby radiosonde

launch site. We also investigate how much the turbulence limits the accuracy of the station position estimates using a simple PPP (Precise Point Positioning) approach. Finally, we present the conclusions in Sec. 5.

2. Theory

2.1. Simulating Tropospheric Delays

The turbulence induced fluctuations in the refractive index of air can be characterized using the Kolmogorov turbulence theory [6]. According to this theory, the spatial variations in refractive index, n, between two points, $\mathbf{r}_i$ and $\mathbf{r}_j$, can be described using a structure function D_n [7–9]:

$$D_n(\mathbf{r}_i, \mathbf{r}_j) = \left\langle [n(\mathbf{r}_i) - n(\mathbf{r}_j)]^2 \right\rangle = C_n^2 \left(\frac{z_i + z_j}{2} \right) \frac{\|\mathbf{r}_i - \mathbf{r}_j\|^{2/3}}{1 + \left(\frac{\|\mathbf{r}_i - \mathbf{r}_j\|}{L} \right)^{2/3}}, \quad (1)$$

where $\langle \cdot \rangle$ denotes expectation value, C_n is the refractive index structure constant, L is the saturation length scale, and z_i the vertical component of $\mathbf{r}_i$. Temporal variations in the refractive index can be described similarly by assuming Taylor's frozen flow hypothesis [10]. This hypothesis assumes that the turbulent structure of the atmosphere is frozen and moves with the air, i.e. $n(\mathbf{r}, t) = n(\mathbf{r} - \mathbf{v}\, t)$ where $\mathbf{v}$ is the wind vector and t the time. The variations in refractive index between location $\mathbf{r}_i$ at time t_i and location $\mathbf{r}_j$ at time t_j can then be described by:

$$\left\langle [n(\mathbf{r}_i, t_i) - n(\mathbf{r}_j, t_j)]^2 \right\rangle = D_n(\mathbf{r}_i - \mathbf{v}\, t_i, \mathbf{r}_j - \mathbf{v}\, t_j). \quad (2)$$

In this work Equivalent Zenith Wet Delays (EZWDs) are simulated, i.e. slant wet delays divided by their corresponding mapping functions. An EZWD l_i^z of a radio signal observed after propagated along the path S_i, is given by:

$$l_i^z = \frac{1}{m_i} \int_{S_i} [n(\mathbf{r}_i(s)) - 1]\, ds = \int_0^\infty [n(\mathbf{r}_i(z)) - 1]\, dz, \quad (3)$$

where m_i is the mapping function between zenith and the elevation angle of the slant path S_i. Given a known initial EZWD l_0^z in some direction and at some time instant, (like the zenith wet delay at time zero), we can calculate the covariance between two EZWDs, l_i and l_j, given by:

$$[C]_{ij} = \left\langle (l_i^z - l_0^z) \left(l_j^z - l_0^z \right) \right\rangle = \int_0^\infty \int_0^\infty [D_n(\mathbf{r}_i(z), \mathbf{r}_0(z')) + D_n(\mathbf{r}_j(z), \mathbf{r}_0(z')) - D_n(\mathbf{r}_i(z), \mathbf{r}_j(z')) - D_n(\mathbf{r}_0(z), \mathbf{r}_0(z'))]\, dz dz'. \quad (4)$$

Calculating this for every pair of EZWDs we want to simulate, we obtain a covariance matrix C. Since C is symmetric we can perform a Cholesky decomposition [11]:

$$C = DD^T. \quad (5)$$

A vector of simulated EZWDs, $\mathbf{l}^z$, can then be obtained by [1]:

$$\mathbf{l}^z = l_0^z + D\,\mathbf{n}, \tag{6}$$

where $\mathbf{n}$ is a vector of zero-mean Gaussian distributed random numbers with variance 1.

For the simulations we need the profile of C_n, the wind velocity, and the initial EZWD l_0^z. For the structure constant, an often used approximation is to assume that C_n is constant up to an effective tropospheric height H and zero above [9]. This approximation was for example used in the simulations in [1]. In this work we simulate EZWDs using both this approximate model and using vertical C_n profiles estimated from high resolution radiosonde data.

2.2. Estimating the Structure Constant from Radiosonde Data

The structure constant C_n can be estimated from radiosonde data. The method used in this work is described in, for example, [2–5]. It is briefly summarized below.

The mixing of the air inside a turbulent eddy will cause any large scale gradient in the refractive index to be mixed into creating small scale refractive index fluctuations. By knowing the size of the large scale gradient and the typical mixing distance the magnitude of the fluctuations, i.e. C_n^2, can be estimated. The typical mixing distance is related to the so called *outer scale of atmospheric turbulence*, L_0. C_n^2 can be estimated by:

$$C_n^2 = a^2 \left\langle L_0^{4/3} \right\rangle F\,M^2, \tag{7}$$

where $a^2 \approx 2.8$, F is the fraction of the air that is turbulent, and M the vertical potential refractive index gradient. The outer scale is normally not known exactly, but its expectation value can be calculated by assuming that L_0 is uniformly distributed between some minimum and some maximum values, for example between 3 m and 100 m [4]. The potential refractive index gradient M is not the full vertical gradient of the refractive index; it only contains the part caused by the gradients in quantities conserved under adiabatic motion in the atmosphere, i.e. the potential temperature θ and the specific humidity q (these are only conserved when there are no clouds, hence the method can only be used under cloud free conditions). Thus, M is calculated by:

$$M = \frac{\partial n}{\partial \theta}\frac{\partial \theta}{\partial z} + \frac{\partial n}{\partial q}\frac{\partial q}{\partial z}. \tag{8}$$

When estimating the derivatives using radiosonde data it is important to remember that only the large scale gradients in θ and q should by considered, not the small scale fluctuations due to turbulence. Hence the gradients should be calculated using data obtained at a vertical sampling larger than L_0 where

the gradient can be assumed larger than the turbulent fluctuations. However, the sampling needs to be small enough that the large scale variations in θ and q can be described by a first order Taylor expansion. In this work we use a sampling distance of 150 m.

The intermittency factor F is required to take into account that only some layers of the atmosphere may be turbulent, while other layers may be non-turbulent or in a state where they fluctuates between a turbulent an a non-turbulent state. Typically $F \approx 0.1$ [2], however it can vary in time and with height. It is possible to estimate F using statistical methods:

$$F = \int_{S_c}^{\infty} p_S(S) dS, \tag{9}$$

where $S = \left\| \frac{\partial \mathbf{v}}{\partial z} \right\|$ is the wind shear, p_s the probability density function of S, and S_c the wind shear required to make the Richardson number equal to the critical Richardson number [3]. Typically the following expression for p_S is used [3, 4]:

$$p_S(S) = \frac{S}{\sigma_S^2(z)} exp\left(-\frac{S^2 + \langle S(z) \rangle^2}{2\sigma_S^2(z)} \right) I_0\left(\frac{S \langle S(z) \rangle}{\sigma_S^2(z)} \right), \tag{10}$$

where $\langle S(z) \rangle$ is the wind shear estimated using the wind measurements in the radiosonde data, and I_0 is the modified Bessel function of the first order. The parameter $\sigma_S = 0.18\, L_0^{-0.3} \left| \frac{g}{\theta} \frac{\partial \theta}{\partial z} \right|^{0.25} \rho^{-0.15}$, where g is the acceleration due to gravity and ρ the density of the air [4].

3. Examples of C_n^2 Profiles

Fig. 1 shows mean and median C_n^2 profiles estimated from high resolution radiosonde data, for six different locations. As seen, the mean values are typically larger than the median ones, meaning that the distribution for C_n^2 is not symmetrical (probably it is log-normal [4]). We can also note that the average C_n^2 profiles decay almost exponentially with height, and that C_n^2 usually is larger for the stations closer to the equator.

In Fig. 2 the seasonal variation of C_n^2 is shown. As seen C_n^2 is clearly larger in summer compared to winter, especially at lower altitudes. The likely reason is that there is more water vapor in the atmosphere in the summer. The result with higher C_n in summer is in agreement with the results in [12], where slant wet delays inferred from microwave radiometer data were used to estimate C_n. We can also see that there are large variations also over short time scales, of the order of days or shorter.

4. Simulations

We made simulations for the VLBI station Gilmore Creek, Alaska, for the continuous VLBI campaign CONT05. The structure constant profiles used in

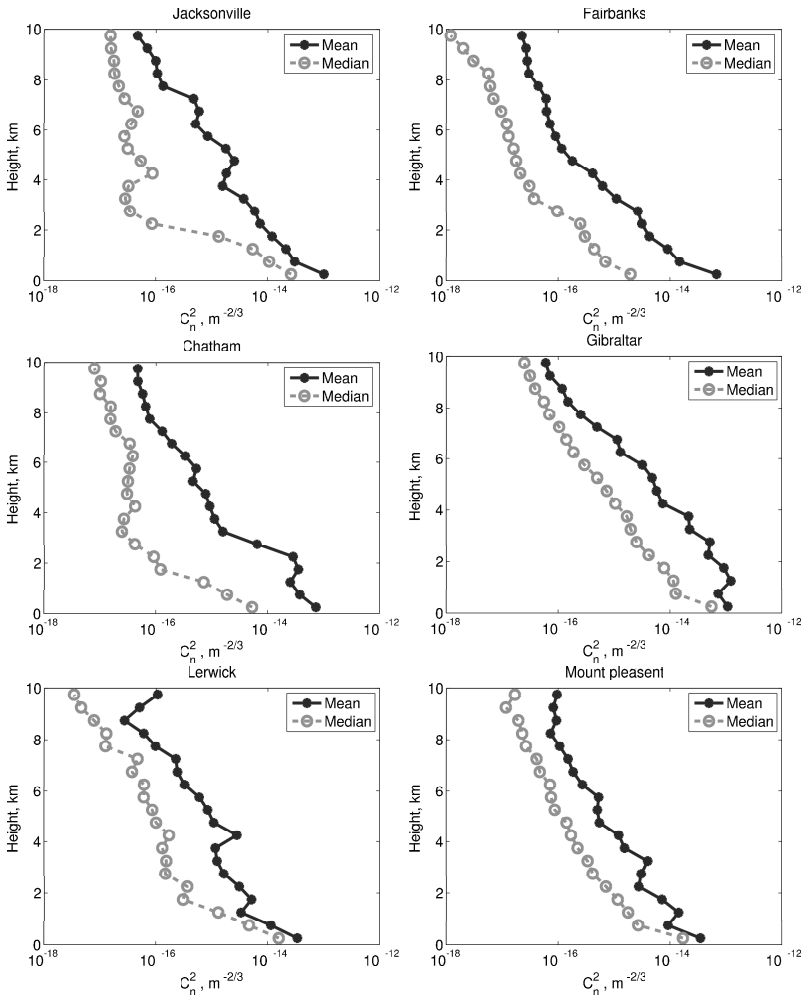

Figure 1. Mean and median C_n^2 profiles for 2005 estimated from radiosonde data

the simulations were those estimated from the nearby radiosonde launch site in Fairbanks, located 30 km away from the VLBI station. From the radiosonde data, there were five different C_n^2 profiles that could be used during the period Sep. 12–28, 2005. The C_n^2 profiles at times in between two radiosonde launches were estimated by linear interpolation of the C_n^2 profiles estimated from the radiosonde data. The wind speed data were obtained from ECMWF data [13]. We made the approximation that the wind speed and direction were constant with height (equal to the ECMWF wind data at the 850 hPa level), but varying with time.

We also made simulations using the simplifying assumption of a constant C_n up to an effective tropospheric height H and zero above. The effective

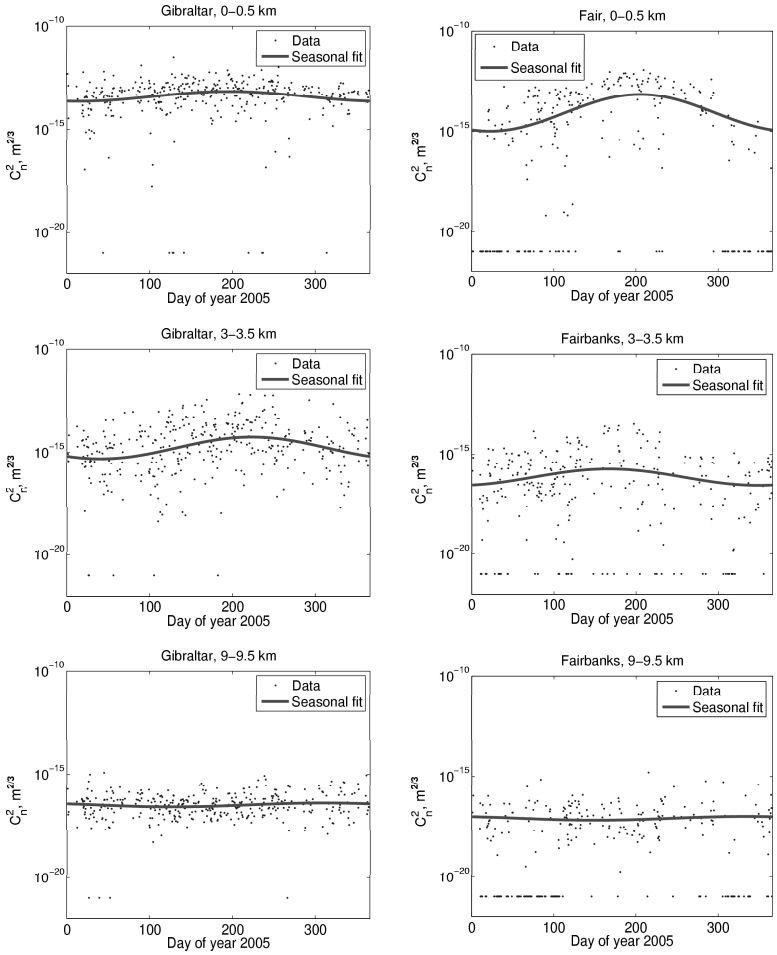

Figure 2. Seasonal variations in C_n^2 observed at Gibraltar and Fairbanks

tropospheric height were estimated as the scale height of the C_n profile, i.e. it was obtained by fitting $\log(C_n(z))$ to the model $\log(C_n(z)) = A - z/H$. The constant C_n value was then estimated so that $C_n \cdot H$ would be equal to the the integral of the mean C_n profile for the CONT05 period. The obtained parameters were H =3170 m and C_n=0.9·10^{-7} m$^{-1/3}$. The wind speed and direction used in these simulations were constant both in time and with height (equal to the mean speed and direction for the period as given by ECMWF for the 850 hPa level).

To investigate the effect the seasonal variations of C_n^2 have on the results, we also made simulations using the C_n^2 profiles obtained in the period Mar. 12–28, 2005 (i.e. six months before CONT05).

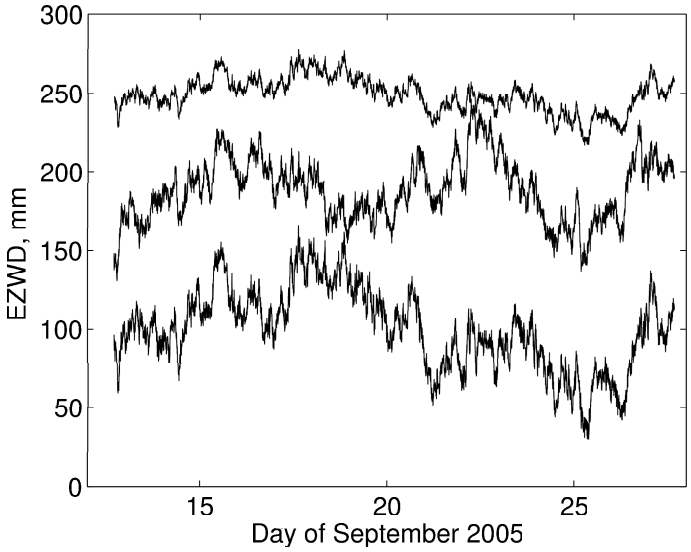

Figure 3. Simulated EZWD for Gilmore Creek during the CONT05 campaign. Shown are delays simulated using C_n profiles estimated using radiosonde data (lower line), as well as delays simulated using constant C_n up to an effective tropospheric height and zero above (middle line, offset by 50 mm), and delays simulated using C_n profiles from March 2005 (upper line, offset by 150 mm)

The time-series of the simulated EZWDs are shown in Fig. 3. The azimuth and the elevation angles of the simulated EZWDs are those observed by the Gilmore Creek VLBI telescope during CONT05. The same random numbers were used in the simulation using the C_n profiles from the radiosonde data and for the simulation using the simplification with constant C_n up to the height H. We can observe that the variations in these time-series look rather similar. However, for the simulations using the data from March 2005, the variations are smaller, a result of smaller C_n in March compared to Sep.

To test how the turbulence affects the accuracy of the position estimates, we used the simulated delays in a simple Precise Point Positioning (PPP) processing. In the PPP processing we made one solution for each one day period. For each day the station position, station clock error (modeled as a second degree polynomial), zenith wet delay (modeled as piecewise linear function in one hour intervals), and tropospheric gradients (modeled as piecewise linear functions in two hour intervals) were estimated. No other error source than the tropospheric delay were simulated.

The obtained repeatabilities for the coordinates are shown in Fig. 4. We can see that the coordinate errors for the simulations using the advanced approach (i.e. using the C_n profiles) and using the simpler approach are similar. When using the advance approach the RMS repeatabilities for the whole period were 1.3 mm, 1.3 mm, and 4.1 mm for the north, east, and vertical component

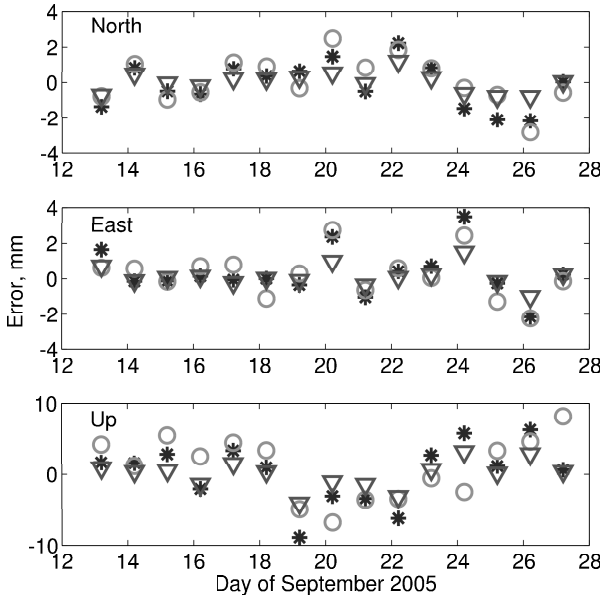

Figure 4. Station position repeatabilities. Shown are the results from the simulations using the advanced approach ($*$), the simplified approach ($\circ$), and the advance approach but using C_n from March 2005 ($\bigtriangledown$)

respectively. The same values when using the simpler approach were 1.3 mm, 1.3 mm, and 4.4 mm, i.e. hardly any differences at all. For the simulation using C_n profiles from March 2005 the repeatabilities are significantly better: the RMS values for these simulations were 0.5 mm, 0.6 mm, and 1.9 mm respectively.

5. Conclusions

Atmospheric turbulence causes fluctuations in the atmospheric delay of the VLBI signals, both as function of time and as function of direction. Since the models used in the processing of VLBI data cannot describe these fluctuations properly, it will cause errors in the parameters estimated in the VLBI analysis. For example, as seen for the simulations presented in this work the error in the estimated vertical coordinates can be several millimeters. The error is season dependent since the structure constant C_n has a seasonal variation.

The C_n profile can be estimated using high resolution radiosonde data. It should however be noted that there is some uncertainty in the C_n profiles estimated using this method. For example, the L_0 value is normally not known very well. In this work we assumed L_0 to be uniformly distributed between

3 m and 100 m, however the maximum and minimum values can be different for different location. In [3] the range 30 m to 100 m is given for the maximum L_0 value. If we would use 30 m instead of 100 m as the maximum value of L_0 the estimated C_n values would be smaller by about a factor 2. More research is needed in order to improve the knowledge about L_0. Another way would be to estimate the C_n profile from the radiosonde data using the alternative approach presented by [5]. That approach however, requires a vertical sampling rate of around 10 m or less (some radiosonde data used in this work only have 50 m sampling), and the method is probably more sensitive to measurement noise in the radiosonde data.

Simplifying the simulations by assuming a C_n constant up to an effective height H and zero above will not affect the simulated delays significantly as long as appropriate C_n and H values are used. Some differences between the simulated time-series using the advanced and simplified approach can be seen. These are likely caused by the fact that there is variations in time in the C_n used in the advanced approach but not in the simplified approach. The repeatabilities obtained from the PPP analysis are similar. It is however important to take into account the seasonal variations of C_n.

The method of simulating atmospheric delays can be used to determine the accuracy that can be reached with space geodetic techniques such as VLBI. For example, the method is presently being used in simulations performed in order to evaluate the performance of the future VLBI system, VLBI2010 [14]. Simulated atmospheric delays can also be used in order to improve the modeling of the atmospheric delays in the VLBI analysis.

Acknowledgements

The radiosonde data used in this work were obtained from the British Atmospheric Data Centre [15] and from the Stratospheric Processes and Their Role in Climate [16] data center. Tobias Nilsson is supported by a grant from the Swedish National Space Board.

References

[1] Nilsson, T., R. Haas, G. Elgered. Simulations of atmospheric path delays using turbulence models. Proc. of the 18th EVGA Working Meeting. J. Böhm, A. Pany, H. Schuh (eds.), 2007, 175–180;
http://mars.hg.tuwien.ac.at/evga/proceedings/S64_Nilsson.pdf.

[2] VanZandt, T.E., J.L. Green, K.S. Gage, et al. Vertical profiles of refractivity turbulence structure constant: Comparison of observations by the Sunset Radar with a new theoretical model. Radio Sci., v. 13, No 5, 819–829, 1978.

[3] d'Auria, G., F.S. Marzano, U. Merlo. Model for estimating the refractive-index stucture constant in clear-air intermittent turbulence. Applied Optics, v. 32, 2674–2680, 1993.

[4] Vasseur, H. Prediction of tropospheric scintillation on satellite links from radiosonde data. IEEE Trans. Antennas Propag., v. 47, No 2, 293–301, 1999.

[5] Nilsson, T. Measuring and modelling variations in the distribution of atmospheric water vapour using GPS. Ph.D. dissertation. Chalmers University of Technology, 2008;
ftp://gere.oso.chalmers.se/pub/tobias/.

[6] Kolmogorov, A.N. The local structure of turbulence in incompressible viscous fluid for very large Reynolds numbers. Dokl. Akad. Nauk SSSR, v. 30, No 4, 299–303, 1941 (English translation: Proc. R. Soc. Lond. A, 434:9-13).

[7] Tatarskii, V.I. The Effects of the Turbulent Atmosphere on Wave Propagation. Israel Program for Scientific Translations, Jerusalem, 1971.

[8] Ishimaru, A. Wave Propagation and Scattering in Random Media. Academic Press, New York, 1978.

[9] Treuhaft, R.N., G.E. Lanyi. The effect of the dynamic wet troposphere on radio interferometric measurements. Radio Sci., v. 22, No 2, 251–265, 1987.

[10] Taylor, G.I. The spectrum of turbulence. Proc. Roy. Soc. Lond. A, v. 164, No 919, 476–490, 1938.

[11] Press, W.H., S.A. Teukolsky, W.T. Vetterling, et al. Numerical Recipies in C: The Art of Scientific Computing, 2nd ed. Cambridge University Press, Cambridge, 1992.

[12] Nilsson, T., L. Gradinarsky, G. Elgered. Correlations between slant wet delays measured by microwave radiometry. IEEE Trans. Geosci. Remote Sensing, v. 43, No 5, 1028–1035, 2005.

[13] European Centre for Medium Range Weather Forecasts, 2008;
http://data.ecmwf.int/.

[14] Niell, A., A. Whitney, B. Petrachenko, et al. VLBI2010: Current and future requirements for geodetic VLBI systems. International VLBI Service for Geodesy and Astrometry 2005 Annual Report. D. Behrend and K. Baver (eds.), NASA/TP-2006-214136, 2006.

[15] UK Meteorological Office, UK High Resolution Radiosonde Data, British Atmospheric Data Centre, 2008;
http://badc.nerc.ac.uk/data/rad-highres/.

[16] Stratospheric Processes and Their Role in Climate (SPARC) Project, US High Resolution Radiosonde Data, 2008;
http://www.sparc.sunysb.edu/html/hres.html.